

Surrogate optimisation strategies for intraocular lens formula constant optimisation

Achim Langenbucher¹  | Jascha Wendelstein^{1,2}  | Alan Cayless³ | Peter Hoffmann⁴ | Nóra Szentmáry^{5,6}

¹Department of Experimental Ophthalmology, Saarland University, Homburg/Saar, Germany

²Institut für Refraktive- Und Ophthalmochirurgie (IROC), Zurich, Switzerland

³School of Physical Sciences, The Open University, Milton Keynes, UK

⁴Augen- Und Laserklinik Castrop-Rauxel, Castrop-Rauxel, Germany

⁵Dr. Rolf M. Schwiete Center for Limbal Stem Cell and Aniridia Research, Saarland University, Homburg/Saar, Germany

⁶Department of Ophthalmology, Semmelweis-University, Budapest, Hungary

Correspondence

Achim Langenbucher, Department of Experimental Ophthalmology, Saarland University, Kirrberger Str 100 Bldg. 22, 66424 Homburg, Germany.
Email: achim.langenbucher@uks.eu

Abstract

Purpose: To investigate surrogate optimisation (SO) as a modern, purely data-driven, nonlinear adaptive iterative strategy for lens formula constant optimisation in intraocular lens power calculation.

Methods: A SO algorithm was implemented for optimising the root mean squared formula prediction error (rmsPE, defined as predicted refraction minus achieved refraction) for the SRKT, Hoffer Q, Holladay, Haigis and Castrop formulae in a dataset of $N=888$ cataractous eyes with implantation of the Hoya Vivinex hydrophobic acrylic aspheric lens. A Gaussian Process estimator was used as the model, and the SO was initialised with equidistant datapoints within box constraints, and the number of iterations restricted to either 200 (SRKT, Hoffer Q, Holladay) or 700 (Haigis, Castrop). The performance of the algorithm was compared to the classical gradient-based Levenberg-Marquardt algorithm.

Results: The SO algorithm showed stable convergence after fewer than 50/150 iterations (SRKT, HofferQ, Holladay, Haigis, Castrop). The rmsPE was reduced systematically to 0.4407/0.4288/0.4265/0.3711/0.3449 dioptres. The final constants were $A=119.2709$, $pACD=5.7359$, $SF=1.9688$, $-a_0=0.5914/a_1=0.3570/a_2=0.1970$, $C=0.3171/H=0.2053/R=0.0947$ for the SRKT, Hoffer Q, Holladay, Haigis and Castrop formula and matched the respective constants optimised in previous studies.

Conclusion: The SO proves to be a powerful adaptive nonlinear iteration algorithm for formula constant optimisation, even in formulae with one or more constants. It acts independently of a gradient and is in general able to search within a (box) constrained parameter space for the best solution, even where there are multiple local minima of the target function.

KEYWORDS

formula constant optimisation, formula prediction error, lens power calculation, nonlinear iterative algorithm, performance metrics, surrogate optimisation

1 | INTRODUCTION

Optimisation of intraocular lens (IOL) formula constants is still a challenging task in modern cataract surgery (Aristodemou et al., 2011; Langenbucher et al., 2022; Langenbucher, Szentmáry, Cayless, Müller, et al., 2021; Schröder et al., 2016; Zhang et al., 2019). Such formula constants are used to customise a ‘generally valid’ IOL power formula to the characteristics of

a specific lens model, to the measurement devices and techniques, to the characteristics of the patient population, and to the ‘handwriting’ of the surgeon. In most clinical situations, formula constants are optimised only for specific IOL models (the optics and haptics design, material, etc.), and other specific predictors of the refractive outcome, such as the biometer model or the refractometry technique (e.g. refraction lane distance), are not considered.

This is an open access article under the terms of the [Creative Commons Attribution-NonCommercial-NoDerivs](https://creativecommons.org/licenses/by-nc-nd/4.0/) License, which permits use and distribution in any medium, provided the original work is properly cited, the use is non-commercial and no modifications or adaptations are made.

© 2024 The Authors. *Acta Ophthalmologica* published by John Wiley & Sons Ltd on behalf of Acta Ophthalmologica Scandinavica Foundation.

In general, formula constant optimisation requires a full set of biometric data used by the calculation scheme to derive the appropriate lens power, the labelled power of the implanted IOL and the postoperative refraction (manual refraction at least 4 weeks after surgery) (Langenbacher et al., 2022; Langenbacher, Szentmáry, Cayless, Müller, et al., 2021). As yet, there is no established standard for formula constant optimisation. For IOL formulae based on a single constant (e.g. the SRKT formula), in most cases, the formula is reversed and solved for the formula constant, and for each datapoint in the dataset considered for constant optimisation, an individual formula constant is derived. From the distribution of all the individual formula constants in the dataset, any statistical metric is extracted (e.g. the arithmetic mean or median) and defined as the optimised formula constant (Langenbacher et al., 2022, 2023a; Langenbacher, Szentmáry, Cayless, Müller, et al., 2021; Schröder et al., 2016).

However, such strategies have major drawbacks: firstly, they are restricted to IOL formulae with a single formula constant, and in formulae with two or more constants (e.g. the Haigis formula), other strategies are required. Secondly, using a statistical metric for the individual constants allows the extraction of the 'best' constant by statistical definition, but this may not be the formula constant that provides the best outcome for the patient in terms of postoperative refraction. Especially where the distribution of individual constants derived from all clinical cases is in some way skewed, this means that metrics such as the mean value of the individual constants do not provide the best solution (Langenbacher, Szentmáry, Cayless, Müller, et al., 2021; Schröder et al., 2016).

Today, most studies dealing with the refractive outcome after cataract surgery aim to optimise formula constants to achieve zero mean refraction in the study population (Aristodemou et al., 2011; Hoffer & Savini, 2021; Zhang et al., 2019). However, even with simple first-generation formulae such as the SRKT, there is no algebraic method to optimise the formula constant, and trial and error methods are used to find the value corresponding to zero mean refractive error (Langenbacher, Szentmáry, Cayless, Müller, et al., 2021; Zhang et al., 2019).

Such tasks are the domain of modern nonlinear iterative optimisation strategies, which enable IOL formula constants to be optimised on a dataset for any target parameter and any target metrics. This means that these strategies could easily be applied to formulae with one or more formula constants, using the refractive outcome as the target parameter with the most relevance for both patient and surgeon. Any statistical metrics such as the mean, mean absolute, root mean squared error (or others) can be used with these methods (Langenbacher et al., 2022, 2023a; Langenbacher, Szentmáry, Cayless, Müller, et al., 2021).

Some of these nonlinear iterative techniques require internal information on the IOL formula, for example, the gradient and/or Hessian matrix of the formula (solved for the target parameter refraction) with respect to the formula constant(s) (Langenbacher et al., 2023a). However,

in the last two decades, increasingly more purely data-driven optimisation techniques, such as Particle Swarm optimisation (Langenbacher et al., 2023b), have been developed in the domain of machine learning. In contrast to the well-established nonlinear iterative techniques such as the Gauss-Newton (Coleman & Li, 1994), Levenberg-Marquardt, Trust-region reflective (Conn et al., 2000) or interior point method (Boyd & Vandenberghe, 2004; Coleman & Li, 1994; Dikin, 1967; Karmarkar, 1984; Press et al., 2007), all of which use the gradient and Hessian matrix to identify the step direction and size during iterations, the data-driven methods based on statistical models are capable of dealing with black box implementations of the formula (Langenbacher et al., 2023a). This means that we require only a module that outputs the predicted refraction when entering the biometric measures and the IOL power.

The purpose of the present study is

- to introduce the surrogate optimisation algorithm as a purely data-driven method to optimise formula constant(s) for arbitrary formulae (even with black box implementations) for any target parameter and any metrics,
- to implement this algorithm in the interpreted language MATLAB, and
- to evaluate the optimisation results and the performance based on a large clinical dataset of patients treated with one IOL model, containing preoperative biometric data, the labelled power of the implanted lens and the postoperative manual refraction.

2 | MATERIALS AND METHODS

2.1 | Dataset for formula constant optimisation

In this retrospective cross-sectional study, we analysed a dataset containing measurements from 888 eyes from a cataract population from Augen- und Laserklinik Castrop-Rauxel, Castrop-Rauxel, Germany. As transferred to us, the dataset contained results from 490 right eyes and 398 left eyes (495 female and 393 male). The mean age was 71.2 ± 9.1 years (median: 71 years, range: 47–91 years). The local ethics committee (Ärztchamber des Saarlandes, registration number 157/21) provided a waiver for this study, and informed patient consent was not required. The data were transferred to us in an anonymised fashion, precluding back-tracing of the patient. The anonymised data contained preoperative biometry derived with the IOLMaster 700 (Carl-Zeiss-Meditec, Jena, Germany), including axial length AL in mm, central corneal thickness CCT in mm, phakic anterior chamber depth ACD in mm measured from the corneal epithelium to the anterior apex of the crystalline lens, central thickness of the crystalline lens LT in mm and corneal front surface radii measured in the flat (R1 in mm) and in the steep meridian (R2 in mm). In all cases, a Vivinex 1 piece hydrophobic aspherical (aberration correcting) monofocal intraocular lens (Hoya Surgical Optics, Singapore) was implanted. In addition, the labelled refractive power

of the inserted lens (PIOL in dpt) and the postoperative refraction (sphere and cylinder both in dpt) 5–12 weeks after cataract surgery were measured by an experienced optometrist and recorded in the dataset. To ensure reliable postoperative refraction, the dataset included only data with a postoperative Snellen decimal visual acuity of 0.8 (20/25 Snellen lines) or higher. The descriptive data on pre-cataract biometry, PIOL and postoperative refraction are summarised in Table 1.

The anonymised Excel data (.xlsx-format) was imported into MATLAB (Matlab 2021a, MathWorks, Natick, USA) for further processing.

2.2 | Preprocessing of the data

Custom software was written in MATLAB. The patient's age was derived from the date of cataract surgery and the date of birth. The mean corneal front and back surface radius of curvature Rmean was calculated as $R_m = 0.5 \cdot (R_1 + R_2)$. To derive the mean corneal power, R1 and R2 were converted to refractive power using the respective keratometer index n_K mentioned in the IOL formula ($K_1 = (n_K - 1)/R_1$ and $K_2 = (n_K - 1)/R_2$) and averaged ($K_{mean} = 0.5 \cdot (K_1 + K_2)$). As some formulae (e.g. SRK/T formula) deal with the corneal radius reconverted from Kmean, we additionally calculated $R_{mean_K} = 0.5 \cdot R_1 \cdot R_2 / (R_1 + R_2)$. The spherical equivalent refraction SEQ was derived as $SEQ = \text{sphere} + 0.5 \cdot \text{cylinder}$.

2.3 | IOL formulae under test

The following lens power calculation formulae were considered in our study:

- SRKT formula published by Sanders, Retzlaff and Kraff (Retzlaff et al., 1990; Sanders et al., 1990),
- Hoffer Q formula published by Hoffer (1981, 1993, 2007),
- Holladay 1 formula published by Holladay and Prager (Holladay et al., 1988),
- Haigis formula (Haigis et al., 2000), and the
- Castrop formula (Langenbucher, Szentmáry, Cayless, Weissensee, et al., 2021; Wendelstein et al., 2022).

The SRKT formula considers the AL and R_{mean_K} (keratometer index $n_K = 1.3375$) together with the formula

constant A; the Hoffer Q formula uses the AL and Kmean (keratometer index $n_K = 1.3375$) together with the formula constant pACD and the Holladay 1 formula considers the AL and the R_{mean_K} (keratometer index $n_K = 4/3$) together with the formula constant SF. The Haigis formula considers the AL, ACD and Rmean together with a formula constant triplet $a_0/a_1/a_2$. The three formula constants are used in terms of a multilinear regression to calculate the ELP as $ELP = a_0 + a_1 \cdot ACD + a_2 \cdot AL$. The keratometer index used in the Haigis formula is $n_K = 1.3315$. The Castrop formula considers the AL, CCT, ACD, LT, Rmean and the corneal back surface radius together with a formula constant triplet C/H/R. For simplicity (as outlined in Langenbucher et al., 2022, 2023a), the measurement of the corneal back surface radius was replaced by $0.834 \cdot R_{mean}$ and CCT was preset to 0.55 mm. The formula constants C and H are used in terms of a multilinear regression to calculate the ELP, and R is used as an offset in the formula predicted refraction to account, for example for the refraction lane distance. The axial length is linearly transformed using a sum-of-segments concept according to Cooke & Cooke (2019a, 2019b). The corneal refractive index used in the Castrop formula is $n_C = 1.376$.

All formulae included in this analysis were reorganised and solved for the SEQ as a function of preoperative biometrical data and PIOL. The formula prediction error PE was defined as the difference between the formula predicted refraction and the SEQ from the postoperative follow-up examination. For the surrogate formula constant optimisation method (Cruz et al., 2022; Forrester et al., 2008; Forrester & Keane, 2009; Gorissen et al., 2010; Johnson et al., 2019; Moeini et al., 2023; Wang et al., 2014; Zhang et al., 2022), the root mean squared PE (rmsPE) was used as an objective function to be minimised globally within the boundaries (Boyd & Vandenberghe, 2004; Mezura-Montes & Coello Coello, 2011; Zhang et al., 2022). An internal function code was programmed to calculate the rmsPE for the input parameters (AL, CCT, ACD, LT and $R_{mean}/K_{mean}/R_{mean_K}$) a function of the formula constants $A/pACD/SF/a_0, a_1, a_2/C, H, R$.

2.4 | Surrogate optimisation for formula constants

Surrogate model based optimisation is a very modern technique of active learning used in engineering and advanced statistics (Cruz et al., 2022; Forrester et al., 2008;

TABLE 1 Descriptive statistics of the dataset with arithmetic mean, standard deviation (SD), median and the lower (quantile 2.5%) and upper (quantile 97.5%) boundary of the 95% confidence interval.

N=888	AL in mm	ACD in mm	LT in mm	Rmean in mm	Kmean in dpt	PIOL in diopters	SEQ in diopters
Mean	24.0980	3.1864	4.6176	7.7666	43.5180	20.6222	-0.5612
SD	1.40721	0.4081	0.4568	0.2682	1.5006	3.7318	0.9236
Median	23.9026	3.1848	4.5929	7.7654	43.4763	21.0000	-0.2500
Quantile 2.5%	21.6757	2.3720	3.7333	7.2702	40.6567	12.0000	-2.2500
Quantile 97.5%	27.3514	3.9435	5.5192	8.3029	46.4324	27.5000	0.5000

Note: AL refers to the axial length, ACD to the external phakic anterior chamber depth measured from the corneal epithelium to the front apex of the crystalline lens, LT to the central thickness of the crystalline lens, Rmean (mean of the flat and steep meridians) to the mean radius of curvature and Kmean (mean of the flat and steep meridians each converted to dioptric power using a keratometer index $n_K = 1.3375$) for the corneal front surface, PIOL to the refractive power of the intraocular lens implant and SEQ to the spherical equivalent power achieved 5–12 weeks after cataract surgery.

Forrester & Keane, 2009; Gorissen et al., 2010; Johnson et al., 2019; Moeini et al., 2023; Wang et al., 2014; Zhang et al., 2022), and machine learning to find optimal design parameter combinations in terms of minimising (or maximising) an objective function globally over a restricted parameter space (Mezura-Montes & Coello Coello, 2011). The parameter space has to be restricted using boundaries, and in most cases box constraints are used. Instead of raster-based scanning through the entire parameter space with a dense grid which consumes lots of computation capacity and time especially in higher dimensional tasks, surrogate optimisation is initialised with a set of starting points and successively adds locations in the parameter space to find the best parameter solution (Gorissen et al., 2010). In addition to the boundaries of the parameter space, surrogate optimisation shows the unique feature of dealing with quantised parameters in the parameter space (Forrester & Keane, 2009). This means that if the formula constants are restricted to a specific precision (e.g. to 2 decimal places) we do not have to round the results accordingly (which is not necessarily the best solution). Instead, the solutions can be restricted to those in a specific raster (Forrester et al., 2008; Forrester & Keane, 2009). A surrogate model is a statistical model that can accurately approximate the output of a function from the input data. In general such a model could 'replace' a complex objective function and is much faster in computation as compared to the evaluation of the objective function itself.

For a detailed explanation of the working principle of surrogate optimisation, we refer to the literature (Cruz et al., 2022; Forrester et al., 2008; Forrester & Keane, 2009; Gorissen et al., 2010; Johnson et al., 2019; Moeini et al., 2023; Wang et al., 2014; Zhang et al., 2022). In general, surrogate optimisation is always based on a surrogate model (Figure 1). First, we need a set of training data. This means that for initialisation, the objective function should be evaluated in a small set of (intelligently selected) locations in the parameter space (the space of formula constants). In the next step, a statistical model is designed to predict the objective function values within the parameter space based on the training data. Such statistical models include more or less all types of machine learning predictors, such as polynomial regressions, support vector machines, Gaussian Process (GP) estimators or neural networks.

Once the initial surrogate model is trained, the optimisation process starts. As the reliability of the optimisation depends on the accuracy of the underlying surrogate model, the design of the model should be selected carefully to accurately predict the behaviour of the object function in the parameter space in the vicinity of the minimum of the objective function. In the next step, the active learning process starts. By evaluating the prediction uncertainty of the model, the dataset is adaptively enriched by adding data points in the parameter space to improve prediction accuracy in the region of the expected minimum of the objective function. This presupposes that the model design is able to predict its own prediction uncertainty in terms of variance or standard deviation. Only those regions in the parameter space

where the model is not confident with its prediction (high variance) require further exploration by adding data points. In other regions of the parameter space where the model feels confident or where the minimum of the objective function is not expected, no further exploration is required.

For this purpose we used a GP estimator design for the surrogate model as this family of statistical models is known to perform pretty well even on a small set of training samples. Furthermore, this model assigns a normal distribution enabling direct extraction of the model prediction value and the variance indicating the uncertainty at each data point.

The next step defines the potential for improvement. From the model we extract the predicted minimum value and define the potential for improvement by evaluating the variances of the model over the entire parameter space. In regions of the parameter space where a sufficient portion of the normal distribution (model uncertainty) is located below the model predicted minimum we expect strong potential for improvement, and additional data points are required to refine and enrich the model. In these cases we loop back to the training of the enriched surrogate model. The GP statistical model believes that at location $(.)$ in the parameter space there is some potential for improvement if there is potential of finding a probability $y(.)$ value smaller than the predicted minimum y_{\min} of the current model. Expressed in an improvement function, we use the expectance value $E(I(.))$, where $I(.)$ refers to the $y(.) - y_{\min}$ for $y(.) < y_{\min}$, and 0 elsewhere, and $E(I(.)) = \int I(.) \cdot p(y) dy$ with $p(y)$ as the probability density function of the normal distribution defined by the model predicted value and variance. If we do not find a sufficient portion of the normal distribution located below the model predicted minimum y_{\min} (i.e. $E(I(.))$ below a threshold and we accept the performance of our model) we take this as the 'best model' and the optimised formula constants.

2.5 | Initialization in the present study

For the parameter space we used the following box constraints: SRKT A: 117 to 122, Hoffer Q pACD: 4.5 to 6.0, Holladay SF: 1.0 to 3.0, Haigis a0: -1.5 to 1.5, a1: 0.05 to 0.5, a2: 0.05 to 0.35, Castrop C: 0.2 to 0.5, H: -0.3 to 0.3, R: -0.3 to 0.3 as lower boundaries and upper boundaries, respectively and without loss of generality. Without assuming any prior knowledge about the optimised formula constants, we decided to use equally spaced training samples in the parameter space. Equidistant sample points were used with the SRKT, Hoffer Q and Holladay formulae (each having a single formula constant) within the box constraints in a raster of 0.5. For the Haigis formula equidistant points with steps of 1.0/0.15/0.1 for a0/a1/a2 were used in the 3-dimensional parameter space, giving in total 64 datapoints. For the Castrop formula equidistant points with steps of 0.1/0.2/0.2 for C/H/R were used in the 3-dimensional parameter space, again giving in total 64 datapoints. The number of iterations in the optimisation process was restricted to 200 for the

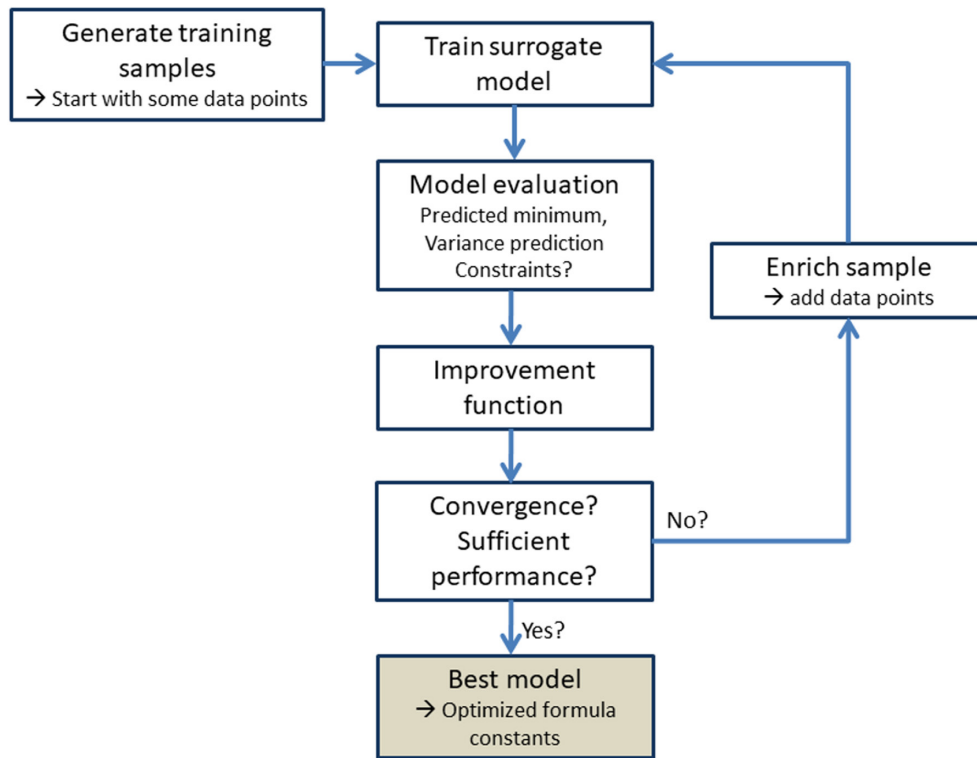


FIGURE 1 Basic strategy behind the surrogate optimisation technique: the surrogate statistical model is trained with some datapoints (training samples). The model is then evaluated and the model prediction, the predicted minimum and the model uncertainty in terms of variance are extracted. In the next step, the improvement function is derived from the model prediction and the uncertainty. If the model shows sufficient performance, we read out the optimised constants otherwise, the model is enriched with additional datapoints and trained again in the loop.

formulae with a single constant and to 700 for those with a constant triplet. The acceptance threshold for $E(I(\cdot))$ was defined as $1e-4$ for all optimisations. To show the benefits of surrogate optimisation in dealing with quantised parameters the optimisation results are shown both without and with quantisation of the formula constants (to 2 decimal places).

2.6 | Explorative data evaluation and statistics

The input data were analysed descriptively in terms of the arithmetic mean, standard deviation, median and the lower and upper boundaries of the 95% confidence interval. The performance of the formula constant optimisation was explored descriptively in terms of the arithmetic mean, standard deviation, median and the lower and upper boundaries of the 95% confidence interval of the formula prediction error PE, together with the mean absolute PE and the rmsPE.

3 | RESULTS

3.1 | Working example for our surrogate optimisation

The principle of surrogate model optimisation is shown in a working example based on our dataset of $N=888$ data for the example of the SRKT formula. We assume the optimised A constant to be located within boundaries from 117 to 122. To show the capabilities of this optimisation technique, four datapoints,

irregularly distributed over the parameter space are used for the initialization of our working example (A: 118.00, 118.50, 118.75 and 121.5) as shown in Figure 2a (upper left graph, red circles). The objective function (root mean squared PE) is evaluated at each of these four datapoints and displayed on the Y axis. The blue line in the graph shows the prediction of the GP model based on the four datapoints, and the dotted magenta lines refer to the model uncertainty derived from the GP model. We see that at the four datapoints, the model feels confident and the uncertainty equals zero, whereas in the intervals between the datapoints, the uncertainty increases with the distance to the closest datapoint. The green interrupted lines refer to the location of the A constant having the best performance, as predicted by the surrogate model. Figure 2b shows the situation of the GP model at the initialisation in more detail: again, the four irregularly distributed datapoints in the parameter space are marked (magenta X together with the model prediction characteristics (green dotted line)). As a result of the uncertainty of the GP model outside the four datapoints, there is some probability for the model to over- or underestimate the performance (colour-coded according to the scale shown on the colour bar on the right side of the graph). For visualisation, the probability $y(A)$ is clipped to a maximum of 5, giving some insight into the distribution (clipped values marked with red dots). The uncertainty of the GP model at all A values is expressed as a normal distribution (dashed red lines), as in the example shown for two datapoints ($A=117.25$ and 119.15). The expectance value $E(A)$ refers to the probability $y(A)$ of obtaining a model performance value better than the

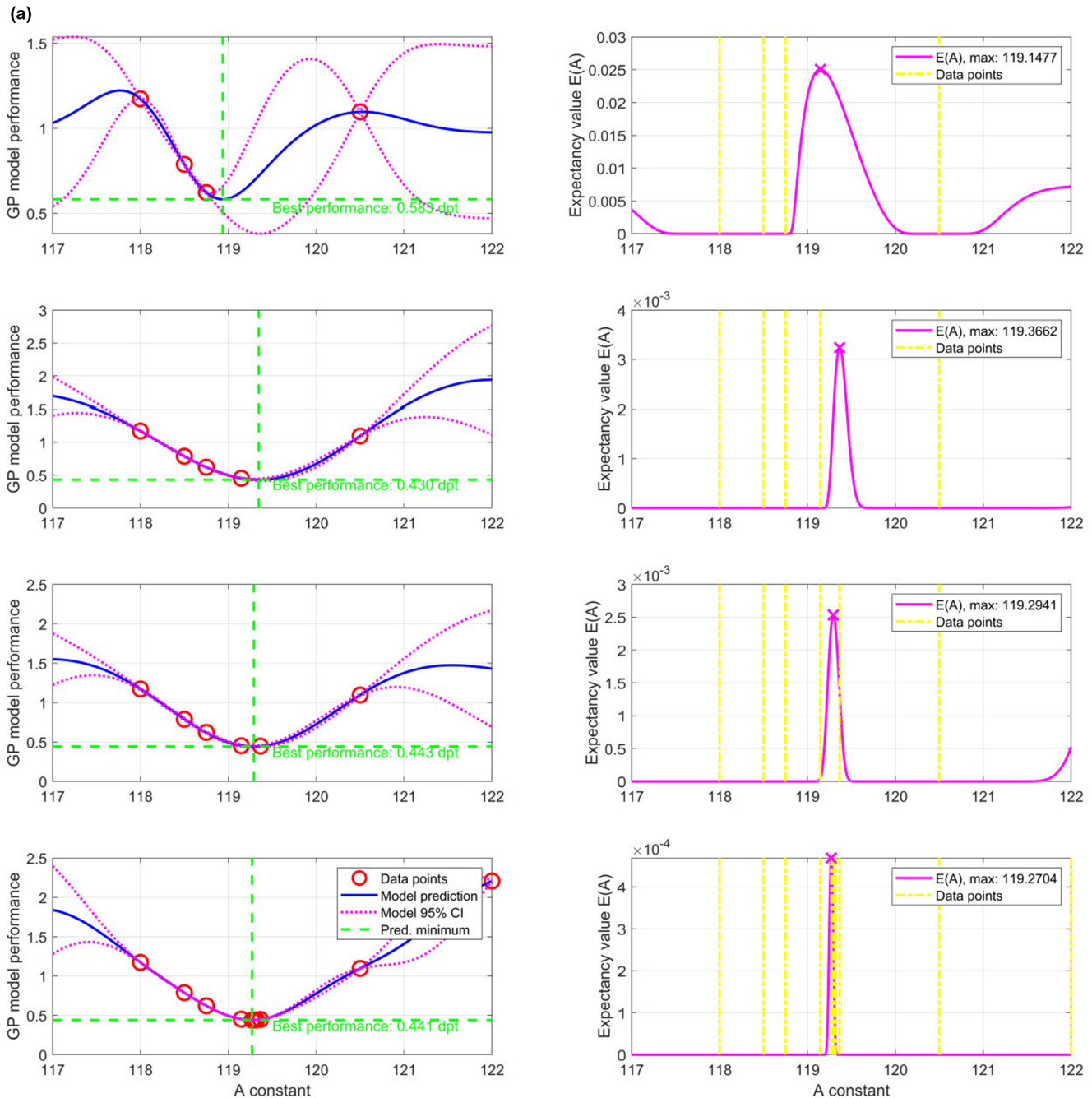


FIGURE 2A Example of the evaluation of the first iterations of the surrogate optimisation process with a Gaussian Process (GP) estimator for the SRKT formula based on our dataset of $N=888$ measurements. 1st row left graph: initialisation with four datapoints (red circles at $A=118.0$, 118.5 , 118.75 and 120.5) with the respective evaluation of the object function (Y axis). The surrogate GP model interpolates between the datapoints and feels confident at the datapoints but shows some uncertainty outside (magenta dotted lines). The best performance predicted by the GP model is marked with dashed green lines (the best performance value mentioned in the graph). 1st row right graph: The potential improvement curve E (cf. Figure 2b) decides whether the model is accepted (E already below the predefined threshold, here $1 \text{ e-}4$) or has to be improved by adding an additional datapoint at the maximum of E . 2nd row: situation at first iteration starting with five datapoints; 3rd row: situation at second iteration starting with six datapoints; and 4th row: situation at 5th iteration starting with nine datapoints. E already dropped to $4.6 \text{ e-}4$.

current predicted best performance, as marked with the cyan dashed line. The portion of the probability $y(A)$ relevant for calculating the expectancy value $E(A)$ is shaded in red. On the upper right graph of Figure 2a, the expectancy value $E(A)$ is shown for the entire range of the A constant within the boundaries (maximum at $A=119.1477$ (magenta X), as indicated in the legend). Starting the optimisation loop, the dataset is enriched by an additional datapoint (now five datapoints) at the maximum of the expectancy function $E(A)$, as shown on the left graph of the second row. We then again search

for the minimum of the model predicted performance (dashed green lines) of the updated model and derive the expectancy function over A (right graph in the second row, maximum value marked with a magenta X). Enriching the dataset again with an additional datapoint at the maximum of $E(A)$ (now six datapoints), we step over to the second iteration, as shown in the 3rd row of graphs. As an example, the situation with five iterations is displayed in the 4th row of Figure 2a. The maximum of the $E(A)$ has already dropped to $4.6 \text{ e-}3$. The iteration is stopped when the maximum of $E(A)$

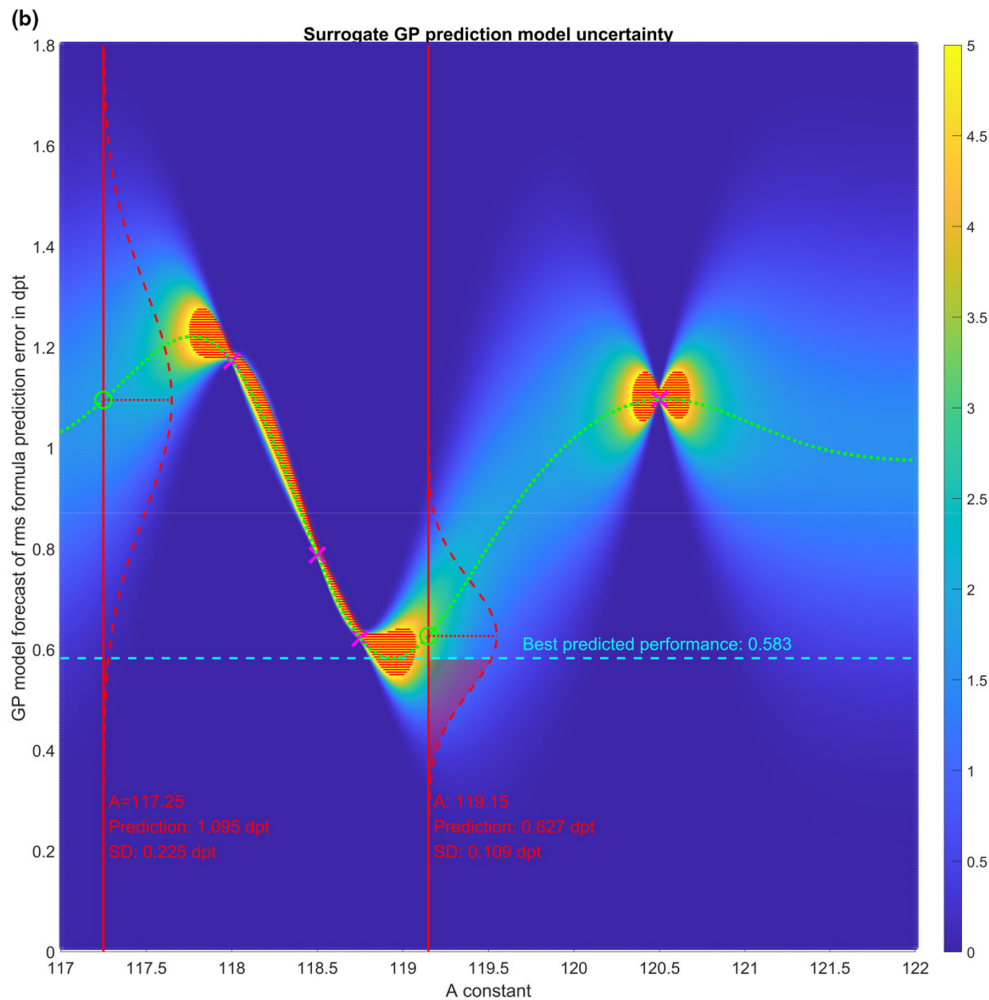


FIGURE 2B Situation of the surrogate Gaussian Process (GP) model after initialisation shown in Figure 2a in more detail: after initialisation with four datapoints (marked with magenta X), the model prediction is shown by the green dotted line and the uncertainty of the model is colour coded according to the colour bar on the right side (clipped to a maximum of five marked with red dots for better visualisation). The model feels confident at the datapoints (uncertainty equals zero), whereas model uncertainty increases with the distance to the closest datapoint. The projected normal distribution of the model's predicted uncertainty is shown for the examples of $A = 117.25$ and $A = 119.15$ (red dashed lines, prediction values and standard deviations (SD) mentioned in the graph). Potential improvement is derived from the best predicted performance (dashed cyan line), the model predicted performance (green dotted line) and the model uncertainty. The highest potential for improvement is detected where the largest portion of the normal distribution (dashed red lines) is below the minimum of the predicted performance curve (dashed cyan line), as indicated by the red-shaded areas.

reaches the threshold of $1e-4$ and the optimised formula constant can then be read out.

For all formulae, the iterative surrogate optimisation process showed convergence on our dataset within the maximum of predefined 200/700 iteration cycles (single constant/triple constant formulae). In Table 2, the optimised formula constants derived from surrogate optimisation are listed for the optimisation without quantisation and also with quantisation to two decimal places. We see that for the formulae with a single formula constant (SRKT, Hoffer Q, and Holladay), rounding the optimised constant to two decimal places gives the same result as independently optimising the formula constants using surrogate optimisation restricted to two decimal places. Conversely, for the formulae with three constants, we find that the optimisation with restriction to two decimal places yields a different formula constant triplet as compared to the rounded constants. With the Haigis formula, a_1 is slightly lower and a_2 is slightly higher, resulting in

a difference of about 0.2 in a_0 . With the Castrop formula, H is slightly higher and R is slightly lower, and these differences effectively compensate each other in such a way that C matches the rounded C in the optimisation without quantisation.

Table 3 displays the results of the performance of all formulae under test with the optimisations without and with quantisation. We see that since the optimisation aims for a minimum rmsPE in the objective function, the mean PE does not exactly reach zero for any formula or any optimisation. Based on our dataset, the performances of the SRKT, Hoffer Q and Holladay formulae are quite similar, with a rmsPE of around 0.43 to 0.44 dpt. However, with the Haigis formula (0.37 dpt) and the Castrop formula (0.34), the respective rmsPE values are lower. The same effect is also observed with the mean absolute PE, where the formulae with a single formula constant range around 0.33 to 0.34, whereas the Haigis formula and the Castrop formula show better performance with values around 0.27 to 0.28.

TABLE 2 Listing of the formula constants for the five formulae under test (SRKT formula with constant A, Hoffer Q formula with constant pACD, Holladay formula with constant SF, Haigis formula with constant triplet a0/a1/a2 and Castrop formula with constant triplet C/H/R) derived with the surrogate optimisation technique.

N = 888	Optimised formula constants without quantisation	Optimised formula constants with quantisation
SRKT	119.2709	119.27
Hoffer Q	5.7359	5.74
Holladay	1.9688	1.97
Haigis a0	-0.5914	-0.88
a1	0.3570	0.35
a2	0.1970	0.21
Castrop C	0.3171	0.32
H	0.2053	0.17
R	0.0947	0.13

Note: Formula constants were optimised independently without quantisation and with quantisation to two decimal places for a dataset of $N=888$ eyes treated with the Hoya Vivinex intraocular lens.

4 | DISCUSSION

Formula constant optimisation using the biometric data and the patient outcome of previous cataract surgeries to improve the outcome of upcoming surgeries still presents a significant challenge. There are currently no universally agreed guidelines or standards as to how formula constants should be optimised. Therefore, in most cases, researchers and clinicians choose the ‘simplest’ way of reversing the IOL power formula to solve for the constant, and then using any established statistical metrics such as mean or median of the distribution on the individual formula constants as an optimised constant in the future (Hoffer & Savini, 2021; Langenbucher et al., 2022; Wang et al., 2017).

We follow a different approach in formula constant optimisation: firstly, we define the formula prediction error as the difference between formula predicted refraction and achieved refraction as the target parameter, since we feel that this measure has the highest relevance for patients and surgeons. Secondly, we define the root mean squared value as the quality metric for this target parameter. To our understanding, this root mean squared value is commonly used in other disciplines (e.g. engineering) as it generally describes the performance much better than the mean or mean absolute value, especially in cases of skewed distributions of the target parameter.

Where the IOL formula is fully disclosed (Savini et al., 2020) and the first and second derivatives with respect to the formula constant(s) can be easily calculated (Rios & Sahinidis, 2013), optimisations based on the gradient (and Hessian matrix) may show the fastest convergence (e.g. the Gauss-Newton or Levenberg-Marquardt method) (Boyd & Vandenberghe, 2004). However, if the objective function rmsPE is complex with more than one minimum, these optimisation techniques could easily become stuck in local minima depending on the initialisation values (Johnson et al., 2019; Zhang et al., 2022). Recently, more and more purely data driven

optimisation strategies have been developed (Rios & Sahinidis, 2013), and most of these techniques have their origins in the artificial intelligence/machine learning domain. Since these data driven techniques do not require any information on the internal workings of the IOL calculation formula itself, we require only a black box implementation (Cruz et al., 2022), effectively giving the refraction prediction as a function of the biometric data and the power of the IOL. This is especially the case for the latest generation formulae which are quite often undisclosed (e.g. the Holladay2, Barrett, or Kane formula) (Savini et al., 2020). Furthermore, these new techniques offer even more advantages over classical nonlinear iteration strategies: firstly, they consider constraints in the parameter space (Forrester et al., 2008; Forrester & Keane, 2009; Mezura-Montes & Coello Coello, 2011), which means that we could choose, for example box constraints to restrict the parameter space to lower and upper limits, or we could use equality or inequality constraints to consider interactions between formula constants (in formulae with more than one constant). Secondly, most of these techniques search over the entire parameter space, which means that they do not become stuck in local minima of the objective function (Gorissen et al., 2010). And third, we could directly consider quantisation in the parameter space, for example if the formula constants are provided with a limited number of decimal places. However, we have to be aware that convergence is typically somehow slower compared to optimisations using the gradient (Boyd & Vandenberghe, 2004; Coleman & Li, 1994; Conn et al., 2000).

In a previous paper, we have already shown the convincing performance of a modern, purely data-driven optimisation strategy called ‘Particle Swarm Optimisation’, (PSO) (Langenbucher et al., 2023b). PSO is initialised with multiple starting points spread over the parameter space of formula constants, together with initial velocities. The positions and velocity vectors are updated in each step depending on metrics such as ‘inertia’, ‘social component’ and ‘cognitive component’.

In the present paper, we present an optimisation strategy that is rather different. Based on a surrogate statistical model, we initially describe the performance of the formula in the parameter space with a model (here a Gaussian Process estimator) based on a couple of points (at which the objective function has to be evaluated, Figure 1). Then we analyse the performance of this model in terms of prediction and uncertainty. In this context, we benefit from the design of a Gaussian Process estimator, as this GP model defines normally distributed uncertainties over the entire parameter space (Forrester et al., 2008). From the prediction and uncertainty behaviour, we define a potential improvement function (in our case, the expectancy value E of receiving a model-predicted objective function lower than the current minimum). At this location, we enrich the (initial) dataset by an additional datapoint and train the model again (Gorissen et al., 2010). We subsequently loop through these steps until we are satisfied with the model performance (e.g. if E falls below a predefined threshold). Once we feel that the model represents the performance sufficiently, we exit the loop, and the minimum

TABLE 3 Performance characteristics (mean, standard deviation, median, 95% confidence interval, mean absolute and root mean squared prediction error [PE]) of the five formulae under test with the constants optimised independently without quantisation and with quantisation to two decimal places (compare Table 2).

N=888		SRKT	Hoffer Q	Holladay	Haigis	Castrop
PE in dpt Optimisation without formula constant quantisation	Mean	0.0061	-0.0366	-0.0201	-0.0043	-0.0050
	Standard deviation	0.4410	0.4275	0.4263	0.3713	0.3450
	Median	-0.0066	-0.0287	-0.0047	0.0078	-0.0058
	2.5% quantile	-0.8816	-0.9285	-0.9323	-0.7839	-0.7109
	97.5% quantile	0.9268	0.8356	0.8106	0.7199	0.6525
	Mean absolute	0.3404	0.3327	0.3265	0.2833	0.2682
	Root mean squared	0.4407	0.4288	0.4265	0.3711	0.3449
PE in dpt Optimisation with formula constant quantisation	Mean	0.0053	-0.0312	-0.0185	-0.0056	0.0008
	Standard deviation	0.4410	0.4280	0.4263	0.3715	0.3451
	Median	-0.0075	-0.0226	0.0028	0.0088	0.0014
	2.5% quantile	0.8823	-0.9252	-0.9310	-0.7954	-0.7041
	97.5% quantile	0.9261	0.8424	0.8120	0.7147	0.6558
	Mean absolute	0.3405	0.3328	0.3265	0.2828	0.2681
	Root mean squared	0.4407	0.4289	0.4265	0.3713	0.3449

Note: Optimisation was performed in terms of minimising the root mean squared PE. The formulae with three constants (Haigis, Castrop) perform better compared to the formulae with a single constant (SRKT, Hoffer Q, Holladay). The optimised formula constants without and with quantisation show similar performance for all metrics.

of the model prediction defines the ‘best solution’ in terms of the optimised formula constants. This strategy is shown for the example of the SRKT formula with a single formula constant (A constant) in Figure 2. Figure 2a shows the situation at the initialisation stage (1st row of graphs), after the first (2nd row) and third iterations (3rd row), and after five iterations (4th row). To show the principle more generally, we restricted the initialisation to four randomly selected datapoints (meaning that we have to evaluate the objective function at 4 of these datapoints) and fitted a GP model to these datapoints. Figure 2b shows the characteristics of the initial model based on these data points in more detail. In addition to the model prediction shown by the dotted green line, the uncertainty in the entire parameter space (range of the A constant) is colour coded, and we see that the model feels most confident at the datapoints where the uncertainty is zero, whereas between the datapoints and to the lower and upper boundaries of the parameter space, the model shows some uncertainty. We then evaluate the probability (normal distribution) that, with the model prediction and uncertainty, we could get a lower model predicted objective function than the actual minimum (extracted from the areas shaded in red). From this analysis, we see the highest potential for improvement at $A = 119.1477$ (rounded to 119.15), and therefore we add a datapoint to the dataset of four datapoints and continue with the first iteration. If we consider the expectancy value at the fifth iteration ($4.6 \cdot 10^{-4}$), we see that we have almost reached the exit criterion for the loop ($1 \cdot 10^{-4}$), and the minimum of the model predicted object function ($A = 119.2707$) is already very close to the final result ($A = 119.2709$).

Overall, the iterative optimisation concept based on a GP surrogate model showed very good performance and strict convergence after a couple of iterations for all formulae under test. The resulting optimised formula constants match the results of previous optimisations using the Levenberg-Marquardt nonlinear iterative

optimisation (Langenbucher et al., 2022, 2023a). Given the option of implementing a quantisation strategy in the optimisation process, we tested the effect of quantisation by restricting the formula constants to a precision of two decimal places. For all formulae under test with a single constant (SRKT, Hoffer Q and Holladay) the optimised constants with quantisation are identical to the directly rounded formula constants optimised without any quantisation, which is not surprising. However, if we optimise the formula constants with quantisation for the Haigis and the Castrop formulae (both based on constant triplets), we obtain slightly different results, and a direct rounding of the formula constants to two decimal places shows some differences in the 2nd digit. This sounds clinically negligible, but directly rounding the result of the constant optimisation without quantisation and calculating the rmsPE results in an rmsPE of 0.3882/0.3455 dpt compared to a rmsPE of 0.3713/0.3449 dpt for the Haigis/Castrop formula, which is slightly higher. This means that if we require formula constants with restrictions to a specific precision (1 or 2 decimal places), we should prefer an optimisation strategy that can deal with quantisation in order to obtain the best solution for the formula constants, especially with the Haigis formula.

However, our study has some limitations: firstly, we restricted the study to four classical and one modern IOL power calculation formulae, and none of the non-disclosed IOL formulae were considered as we do not have any (black box) implementation available. However, we expect that the surrogate optimisation technique could have some benefits, especially in optimising formula constants of non-disclosed formulae, as we do not require insight into the internal workings of the formula and a black box implementation is fully sufficient (Cruz et al., 2022). Secondly, we restricted our surrogate optimisation to a Gaussian Process estimator, as this model directly provides the prediction together with the variance/standard deviation of the model in the entire parameter


space (Rios & Sahinidis, 2013; Wang et al., 2014). Other model designs might also yield proper results in this context (Gorissen et al., 2010). Finally, we performed our calculations on one single dataset from one clinical centre and one lens model. The applicability will be investigated in the future with other large clinical datasets.

In conclusion, we implemented and applied a surrogate statistical Gaussian Process estimator as a modern, purely data-driven adaptive iterative nonlinear optimisation strategy to the problem of formula constant optimisation in cataract surgery. This algorithm starts with some datapoints in the formula constant parameter space defining the initial Gaussian Process model and adaptively improves the performance by stepwise enriching the set of datapoints to increase confidence in the relevant regions of the parameter space where the location of the optimised constants is expected. The algorithm showed proper performance in terms of stable convergence, and the final result was identical to the result of a classical gradient-based algorithm and the Particle Swarm Optimisation as a reference. Further experiments with other datasets and other formulae are required to underline the potential of this algorithm.

ACKNOWLEDGEMENTS

This research received no specific grant from any funding agency in the public, commercial, or not-for-profit sectors. Open Access funding enabled and organized by Projekt DEAL.

ORCID

Achim Langenbacher  <https://orcid.org/0000-0001-9175-6177>

Jascha Wendelstein  <https://orcid.org/0000-0003-4145-2559>

REFERENCES

- Aristodemou, P., Knox Cartwright, N.E., Sparrow, J.M. & Johnston, R.L. (2011) Intraocular lens formula constant optimization and partial coherence interferometry biometry: refractive outcomes in 8108 eyes after cataract surgery. *Journal of Cataract and Refractive Surgery*, 37(1), 50–62. Available from: <https://doi.org/10.1016/j.jcrs.2010.07.037>
- Boyd, S. & Vandenberghe, L. (2004) *Convex optimization*. Cambridge: Cambridge University Press, p. 143.
- Coleman, T.F. & Li, Y. (1994) On the convergence of interior-reflective Newton methods for nonlinear minimization subject to bounds. *Mathematical Programming*, 67, 189–224. Available from: <https://doi.org/10.1007/BF01582221>
- Conn, A.R., Gould, N.I.M. & Toint, P.L. (2000) *Trust-region-methods. MOS-SIAM series on optimization*. Philadelphia, PA: Society for Industrial and Applied Mathematics.
- Cooke, D.L. & Cooke, T.L. (2019a) A comparison of two methods to calculate axial length. *Journal of Cataract and Refractive Surgery*, 45(3), 284–292. Available from: <https://doi.org/10.1016/j.jcrs.2018.10.039>
- Cooke, D.L. & Cooke, T.L. (2019b) Approximating sum-of-segments axial length from a traditional optical low-coherence reflectometry measurement. *Journal of Cataract and Refractive Surgery*, 45(3), 351–354. Available from: <https://doi.org/10.1016/j.jcrs.2018.12.026>
- Cruz, N.C., González-Redondo, Á., Redondo, J.L., Garrido, J.A., Ortigosa, E.M. & Ortigosa, P.M. (2022) Black-box and surrogate optimization for tuning spiking neural models of striatum plasticity. *Frontiers in Neuroinformatics*, 16, 1017222. Available from: <https://doi.org/10.3389/fninf.2022.1017222>
- Dikin, I.I. (1967) Iterative solution of problems of linear and quadratic programming. *Doklady Akademii Nauk SSSR*, 174(1), 747–748.
- Forrester, A.I.J. & Keane, A.J. (2009) Recent advances in surrogate-based optimization. *Progress in Aerospace Sciences*, 45(1–3), 50–79. Available from: <https://doi.org/10.1016/j.paerosci.2008.11.001>
- Forrester, A.I.J., Sobester, A. & Keane, A.J. (2008) *Engineering design via surrogate modelling – a practical guide*. Hoboken, NJ: Wiley.
- Gorissen, D., Couckuyt, I., Demeester, P. & Dhaene, T. (2010) A surrogate modeling and adaptive sampling toolbox for computer based design. *Journal of Machine Learning Research*, 11, 2051–2055.
- Haigis, W., Lege, B., Miller, N. & Schneider, B. (2000) Comparison of immersion ultrasound biometry and partial coherence interferometry for intraocular lens calculation according to Haigis. *Graefes Archive for Clinical and Experimental Ophthalmology*, 238(9), 765–773. Available from: <https://doi.org/10.1007/s004170000188>
- Hoffer, K.J. (1981) Intraocular lens calculation: the problem of the short eye. *Ophthalmic Surgery*, 12(4), 269–272.
- Hoffer, K.J. (1993) The Hoffer Q formula: a comparison of theoretic and regression formulas. *Journal of Cataract and Refractive Surgery*, 19(6), 700–712. Available from: [https://doi.org/10.1016/s0886-3350\(13\)80338-0](https://doi.org/10.1016/s0886-3350(13)80338-0). Erratum. *J Cataract Refract Surg* 1994; 20: 677.
- Hoffer, K.J. (2007) Errors in self-programming the Hoffer Q formula. *Eye (London, England)*, 21(3), 429; author reply 430. Available from: <https://doi.org/10.1038/sj.eye.6702559>
- Basu S. Reply to Dr. Haigis; 21(4):550. Available from: <https://doi.org/10.1038/sj.eye.6702560>
- Hoffer, K.J. & Savini, G. (2021) Update on intraocular lens power calculation study protocols: the better way to design and report clinical trials. *Ophthalmology*, 128, e115–e120. Available from: <https://doi.org/10.1016/j.ophtha.2020.07.005>
- Holladay, J.T., Prager, T.C., Chandler, T.Y., Musgrave, K.H., Lewis, J.W. & Ruiz, R.S. (1988) A three-part system for refining intraocular lens power calculations. *Journal of Cataract and Refractive Surgery*, 14(1), 17–24. Available from: [https://doi.org/10.1016/s0886-3350\(88\)80059-2](https://doi.org/10.1016/s0886-3350(88)80059-2)
- Johnson, A.J., Meyerson, E., de la Parra, J., Savas, T.L., Miikkulainen, R. & Harper, C.B. (2019) Flavor-cyber-agriculture: optimization of plant metabolites in an open-source control environment through surrogate modeling. *PLoS One*, 14(4), e0213918. Available from: <https://doi.org/10.1371/journal.pone.0213918>. Retraction in: *PLoS One* 2021 Oct 25;16(10):e0259294.
- Karmarkar, N. (1984) A new polynomial-time algorithm for linear programming. *Combinatorica*, 4, 373–395. Available from: <https://doi.org/10.1007/BF02579150>
- Langenbacher, A., Szentmáry, N., Cayless, A., Müller, M., Eppig, T., Schröder, S. et al. (2021) IOL formula constants: strategies for optimization and defining standards for presenting data. *Ophthalmic Research*, 64(6), 1055–1067. Available from: <https://doi.org/10.1159/000514916>
- Langenbacher, A., Szentmáry, N., Cayless, A., Weisensee, J., Fabian, E., Wendelstein, J. et al. (2021) Considerations on the Castrop formula for calculation of intraocular lens power. *PLoS One*, 16(6), e0252102. Available from: <https://doi.org/10.1371/journal.pone.0252102>
- Langenbacher, A., Szentmáry, N., Cayless, A., Wendelstein, J. & Hoffmann, P. (2022) Strategies for formula constant optimisation for intraocular lens power calculation. *PLoS One*, 17(5), e0267352. Available from: <https://doi.org/10.1371/journal.pone.0267352>
- Langenbacher, A., Szentmáry, N., Cayless, A., Wendelstein, J. & Hoffmann, P. (2023a) Formula constant optimisation techniques including variation of keratometer or corneal refractive index and consideration for classical and modern IOL formulae. *PLoS One*, 18(2), e0282213. Available from: <https://doi.org/10.1371/journal.pone.0282213>
- Langenbacher, A., Szentmáry, N., Cayless, A., Wendelstein, J. & Hoffmann, P. (2023b) Particle swarm optimisation strategies for IOL formula constant optimisation. *Acta Ophthalmologica*, 101, 775–782. Available from: <https://doi.org/10.1111/aos.15664>
- Mezura-Montes, E. & Coello Coello, C.A. (2011) Constraint-handling in nature-inspired numerical optimization: past, present and

- future. *Swarm and Evolutionary Computation*, 1, 173–194. Available from: <https://doi.org/10.1016/j.swevo.2011.10.001>
- Moieni, M., Yue, L., Begon, M. & Lévesque, M. (2023) Surrogate optimization of a lattice foot orthotic. *Computers in Biology and Medicine*, 155, 106376. Available from: <https://doi.org/10.1016/j.combiomed.2022.106376>
- Press, W.H., Teukolsky, S.A., Vetterling, W.T. & Flannery, B.P. (2007) *Section 10.11. Linear programming: interior-point methods*. In: *Numerical recipes: the art of scientific computing*, 3rd edition. New York, NY: Cambridge University Press.
- Retzlaff, J.A., Sanders, D.R. & Kraff, M.C. (1990) Development of the SRK/T intraocular lens implant power calculation formula. *Journal of Cataract and Refractive Surgery*, 16(3), 333–340. Available from: [https://doi.org/10.1016/s0886-3350\(13\)80705-5](https://doi.org/10.1016/s0886-3350(13)80705-5). Erratum in: *Journal of Cataract and Refractive Surgery* 1990 Jul;16(4):528.
- Rios, L.M. & Sahinidis, N.V. (2013) Derivative-free optimization: a review of algorithms and comparison of software implementations. *Journal of Global Optimization*, 56(3), 1247–1293. Available from: <https://doi.org/10.1007/s10898-012-9951-y>
- Sanders, D.R., Retzlaff, J.A., Kraff, M.C., Gimbel, H.V. & Raanan, M.G. (1990) Comparison of the SRK/T formula and other theoretical and regression formulas. *Journal of Cataract and Refractive Surgery*, 16(3), 341–346. Available from: [https://doi.org/10.1016/s0886-3350\(13\)80706-7](https://doi.org/10.1016/s0886-3350(13)80706-7)
- Savini, G., Taroni, L. & Hoffer, K.J. (2020) Recent developments in intraocular lens power calculation methods-update 2020. *Annals of Translational Medicine*, 8(22), 1553. Available from: <https://doi.org/10.21037/atm-20-2290>
- Schröder, S., Leydolt, C., Menapace, R., Eppig, T. & Langenbucher, A. (2016) Determination of personalized IOL-constants for the Haigis formula under consideration of measurement precision. *PLoS One*, 11(7), e0158988. Available from: <https://doi.org/10.1371/journal.pone.0158988>
- Wang, C., Duan, Q., Gong, W., Ye, A., Di, Z. & Miao, C. (2014) An evaluation of adaptive surrogate modeling based optimization with two benchmark problems. *Environmental Modelling & Software*, 60, 167–179. Available from: <https://doi.org/10.1016/j.envsoft.2014.05.026>
- Wang, L., Koch, D.D., Hill, W. & Abulafia, A. (2017) Pursuing perfection in intraocular lens calculations: III. Criteria for analyzing outcomes. *Journal of Cataract and Refractive Surgery*, 43(8), 999–1002. Available from: <https://doi.org/10.1016/j.jcrs.2017.08.003>
- Wendelstein, J., Hoffmann, P., Hirschall, N., Fischinger, I.R., Mariacher, S., Wingert, T. et al. (2022) Project hyperopic power prediction: accuracy of 13 different concepts for intraocular lens calculation in short eyes. *The British Journal of Ophthalmology*, 106(6), 795–801. <https://doi.org/10.1136/bjophthalmol-2020-318272>
- Zhang, J.Q., Zou, X.Y., Zheng, D.Y., Chen, W.R., Sun, A. & Luo, L.X. (2019) Effect of lens constants optimization on the accuracy of intraocular lens power calculation formulas for highly myopic eyes. *International Journal of Ophthalmology*, 12(6), 943–948. Available from: <https://doi.org/10.18240/ijo.2019.06.10>
- Zhang, L., Xu, Z.J. & Zhang, Y. (2022) Data-informed deep optimization. *PLoS One*, 17(6), e0270191. Available from: <https://doi.org/10.1371/journal.pone.0270191>

How to cite this article: Langenbucher, A., Wendelstein, J., Cayless, A., Hoffmann, P. & Szentmáry, N. (2024) Surrogate optimisation strategies for intraocular lens formula constant optimisation. *Acta Ophthalmologica*, 102, e915–e925. Available from: <https://doi.org/10.1111/aos.16670>